Analytica Chimica Acta 1064 (2019) 33–39

Contents lists available at ScienceDirect

Analytica Chimica Acta

journal homepage: www.elsevier.com/locate/aca

Sensitive electrochemical biosensor for MicroRNAs based on duplex-specific nuclease-assisted target recycling followed with gold nanoparticles and enzymatic signal amplification

Hui Zhang [a, *], Mengxing Fan [a, b], Juqian Jiang [a], Qingming Shen [b, **], Chenxin Cai [a], Jian Shen [a, ***]

[a] Jiangsu Key Laboratory of New Power Batteries, Jiangsu Collaborative Innovation Center of Biomedical Functional Materials, Jiangsu Key Laboratory of Biomedical Materials, National and Local Joint Engineering Research Center of Biomedical Functional Materials, College of Chemistry and Materials Science, Nanjing Normal University, Nanjing, 210023, PR China

[b] Key Laboratory for Organic Electronics and Information Displays & Jiangsu Key Laboratory for Biosensors, Institute of Advanced Materials (IAM), Jiangsu National Synergetic Innovation Center for Advanced Materials (SICAM), Nanjing University of Posts & Telecommunications, Nanjing, 210023, PR China

HIGHLIGHTS

- A triple signal electrochemical biosensor was developed to miRNA-21 detection.
- The triple signal amplification was fulfilled by the DSN assisted target recycling combined with gold NPs, HRP enzymatic signal amplification.
- The biosensor can distinguish similar miRNAs that differ by only one base.
- The biosensor exhibited great precision, high selectivity and good repeatability for miRNA detection.
- The concentration of endogenous miRNA-21 of A549 cells can be detected using this method.

GRAPHICAL ABSTRACT

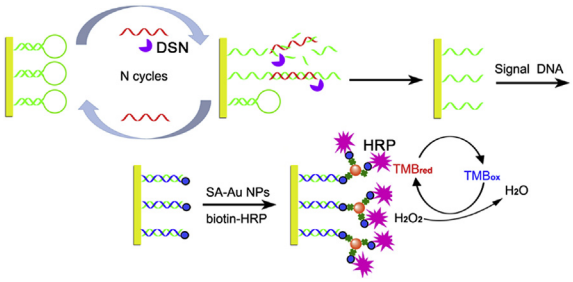

ARTICLE INFO

Article history:
Received 13 December 2018
Received in revised form
20 February 2019
Accepted 26 February 2019
Available online 15 March 2019

Keywords:
Electrochemical biosensor
MicroRNAs
Duplex specific nuclease
Horseradish peroxidase
Signal amplification

ABSTRACT

The detection of sequence-specific microRNAs (miRNAs) is an important factor to the diseases diagnosis. Herein, a triple signal amplification electrochemical biosensor for highly sensitive detection of miRNA-21 was developed based on a duplex-specific nuclease (DSN)-assisted target recycling combined with gold nanoparticles (NPs), horseradish peroxidase (HRP) enzymatic signal amplification. The electrochemical biosensor generated significantly amplified amperometric current changes (Δi) for the detection of miRNA-21 down to 43.3 aM, and Δi was proportional to the logarithm of the concentration of miRNA-21 within the range of 0.1 fM to 100 pM. Meanwhile, the inherent selectivity of the term hairpin capture probe endowed the biosensor with high differentiation of similar miRNAs. The good feasibility of the proposed strategy for cell miRNA detection was confirmed by analyzing miRNA-21 in A549 lysates, which indicates its promising potential in biomedical research and clinical analysis.

* Corresponding author.
** Corresponding author.
*** Corresponding author.
E-mail addresses: zhangh@njnu.edu.cn (H. Zhang), iamqmshen@njupt.edu.cn (Q. Shen), jshen@njnu.edu.cn (J. Shen).

https://doi.org/10.1016/j.aca.2019.02.060
0003-2670/

1. Introduction

MicroRNAs (miRNAs) are small non-coding RNA molecules containing about 18–25 nucleotides which play important roles in several biological processes such as differentiation, metabolic homeostasis, cellular apoptosis and proliferation [1,2]. The dysregulation of miRNA expression is usually related to various human diseases. For example, miRNA-21 plays an important role in the course of oncogenesis. The expression of miRNA-21 is significantly upregulated in different kinds of cancers. It is involved in cell proliferation, cell invasiveness, angiogenesis and other biological functions. Therefore, miRNAs have been regarded as effective biomarker candidates for the diagnosis, classification, prognosis, and treatment response evaluation of cancers [3–7].

Current standard methods of miRNA detection are based on traditional molecular biology techniques, such as the polymerase-chain reaction (PCR) [8], microarrays [9], and Northern blotting [10]. These approaches are reliable but are usually labor intensive, time-consuming, low sensitivity and technically difficult [11–14]. Recently, electrochemical biosensors have attracted growing attention due to their intrinsic advantages, such as high sensitivity, speed, simplicity, and low cost, which are suitable for point-of-care diagnostics and multiplexed platforms [12–15]. A typical nucleic acid electrochemical biosensor is fabricated by an electrode with immobilized single-stranded nucleotide probes for hybridization with the complementary target sequence [16–18]. In the presence of target sequence, the hybridization event can be transduced into a detectable electrochemical signal. Despite the simplicity of the electrochemical biosensor, the application of this type of biosensor is challenged by the low abundance of miRNAs and the high sequence homology among miRNA family members [19–26].

To address these challenges, many signal amplification methods based on the cleavage of nucleases have been developed to detection of miRNAs [27–41]. Among these different nucleases, duplex-specific nuclease (DSN) has attracted increasing interest and become a particularly popular tool in the miRNA detection [30–41]. DSN is a novel and stable nuclease that shows a strong preference for cleaving double stranded DNA or DNA in DNA/RNA hybrid duplexes with at least 15 bp, but it is inactive to single-stranded DNA, RNA or double stranded RNA. Furthermore, this nuclease exhibits good ability to discriminate between perfectly matched and slightly mismatched (up to one mismatch) short duplexes [30–41].

Herein, a highly sensitive and selective electrochemical biosensor was developed to miRNA-21 detection. In this protocol, a DSN assisted target recycling signal amplification strategy was introduced for the sensitive detection of miRNAs (Fig. 1). In the absence of the target miRNAs, DSN is inactive to the hairpin DNA (hDNA) due to the short stems (8 bp) and the steric hindrance of the hairpin structures preventing DSN from accessing the dsDNA stems of the hDNA. When the target miRNAs are incubated with the biosensor, the miRNAs could hybridize with hDNA and unfold the hDNA to form DNA/RNA duplexes. Then, the DNA sequence of the DNA/RNA duplexes could be recognized and selectively cleaved by DSN, resulting in the release of target miRNA. The released target miRNA can be recycled in the next hybridization. Thus, the original detection signal can be amplified exponentially by the DSN-assisted target recycling amplification. In addition to target recycling by DSN, two effective approaches including gold nanoparticles (Au NPs) and horseradish peroxidase (HRP) enzymatic catalysis reaction amplification were also introduced for the fabrication of the sensitive electrochemical assay. The excellent enzymatic activity, combined with the high surface-to-volume ratios and well-controlled surface properties of Au NPs have led to broad application of nanoparticles in biosensors [22,41]. As shown in Fig. 1, in the presence of target miRNA, the complementary unit of the hDNA on the electrode surface hybridizes with target miRNA and forms RNA/DNA duplexes, which become the substrate of the DSN. Since DSN cleaves only the DNA strands in the duplexes, the target miRNA is subsequently released and hybridized with another hDNA. The residual DNA fragment on the electrode hybridizes with the biotin-labeled signal DNA (sDNA). Eventually, one miRNA can lead to the hybridization of a large amount of sDNA. Because sDNA is labeled with biotin, streptavidin (SA)-coated Au NPs are captured on the electrode surface due to the SA/biotin interaction. The numerous SA molecules on the Au NPs can subsequently immobilize a large number of biotin-labeled horseradish peroxidase (HRP) molecules. The Au NPs serve as nanocarriers for HRP and can help to maintain their enzymatic activity. And they also promote electron transfer and assist the

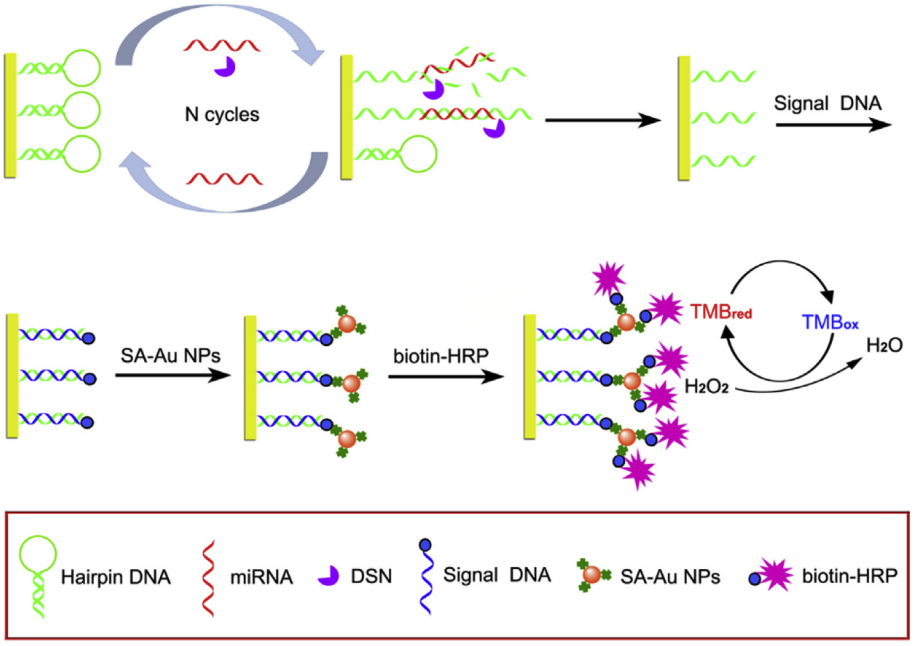

Fig. 1. Schematic illustration of the electrochemical miRNA biosensor based on DSN-assisted target recycling followed with Au NPs and HRP enzymatic signal amplification strategy.

electron transfer between HRP and the gold electrode [42]. Furthermore, HRP can catalyze the reduction of hydrogen peroxide and in the presence of 3,3′,5,5′–tetramethylbenzidine (TMB), electrochemical current signals can be generated, which dramatically amplifies the electrochemical signal [43]. Thus, in this proposed method, the corresponding electrochemical signal activated and enhanced in the presence of target miRNA. In addition, owing to the strong differentiating ability of DSN, the method can distinguish similar miRNAs that differ by only one base. Therefore, the proposed biosensor has great potential as a platform for the highly sensitive and selective detection of miRNAs.

2. Experimental

2.1. Materials and reagents

Tris(hydroxymethyl-1)aminomethane (Tris), Tris(2-carboxyethyl)phosphine hydrochloride (TCEP, 98%), 6-mercapto-1-hexanol (MCH) and streptavidin colloidal gold (SA-Au NPs, 10 nm) were purchased from Sigma-Aldrich Co., Ltd. (St. Louis, MO, USA). Duplex-specific nuclease (DSN) was purchased from Evrogen Co., Ltd. (Moscow, Russia). Biotinylated peroxidase (Biotin-HRP) was supplied by Invitrogen Co., Ltd. (Carlsbad, CA, USA). The TMB substrate (3,3′,5,5′-tetramethylbenzidine) was purchased from Neogen Co., Ltd. (Lexington, KY, USA) in the format of a ready-to-use reagent (K-blue substrate, H_2O_2 included). The other chemicals and reagents were of analytical grade, and obtained from Sinopharm Chemical Reagent Co., Ltd. (Beijing, China). All solutions were prepared with ultrapure water, which was obtained from a Millipore Milli-Q purification system and had an electric resistance >18.3 MΩ. The washing solution was 10 mM Tris-HCl buffer (pH 7.4). The pH values of electrolytes were determined by a 320-S acidity meter (Mettler-Toledo, Switzerland).

The synthetic DNA oligonucleotides were purchased from Sangon Biotechnology Co., Ltd. (Shanghai, China) and purified with high-performance liquid chromatography. All the RNA oligonucleotides were synthesized by TaKaRa Biotechnology Co., Ltd. (Dalian, China). Their base sequences are listed as follows,

Hairpin DNA:

5′-SH-$(CH_2)_6$ *CGAGTC*TAGCCAACATCAGTCTGATAAGCTA*GACTCG*-3′

Signal DNA:
5′-Biotin-GCTAGACTCG-3′
MiRNA-21 (S1):
5′-UAGCUUAUCAGACUGAUGUUGA-3′
One-base mismatched miRNA-21 (S2):
5′-UAGCUUCUCAGACUGAUGUUGA-3′
Three-base mismatched miRNA-21 (S3):
5′-UAACUUAUCACACUGAUAUUGA-3′
Random noncomplementary miRNA (S4):
5′-UGAGGUAGUAGGUUGUGUGGUU-3′

In order to inhibit the effect of RNase on the stability of miRNAs, the solutions and glassware tubes were treated with 0.1% diethylpyrocarbonate (DEPC) and autoclaved. All DNA solutions were prepared with 10 mM Tris-HCl buffer (pH 7.4). The miRNAs solutions were prepared with DEPC-treated water in a RNase-free environment.

2.2. Apparatus

Electrochemical impedance spectroscopy (EIS) was performed on an Autolab PGSTAT302N electrochemical station (Metrohm) at an amplitude of 5 mV in the presence of 5 mM $[Fe(CN)_6]^{3-}$/$[Fe(CN)_6]^{4-}$ solution containing 0.5 M KCl at a 0 V bias potential against the open circuit potential in the frequency range 0.01Hz–100 KHz.

Typical cyclic voltammetry (CV) and amperometric measurements were carried out on a CHI 660E electrochemical workstation (CH Instruments, Shanghai, China) in a conventional three-electrode electrochemical cell with the gold electrode as a working electrode, and a saturated calomel electrode (SCE) and a platinum wire as reference electrode and auxiliary electrode, respectively. Prior to measurements, all solutions were degassed by flowing pure N_2 for 10 min and kept under a N_2 ambient throughout the measurement. CVs were conducted at a scan rate of 100 mV/s. Amperometric measurements were obtained at a fixed potential of 100 mV, and the electrochemical reduction currents were measured after the TMB redox reaction reached steady state.

2.3. Fabrication of the biosensor

A gold disk electrode (2 mm in diameter, CH Instruments) was used as the substrate for immobilizing the hairpin DNA. Prior to use, the electrode was polished and cleaned [44]. For the immobilization of thiol-modified hairpin DNA on the gold electrode surface, 20 μL of hairpin DNA solution (10 μM) with TCEP (10 mM) was first incubated for 1 h to reduce the disulfide bond. By incubating the resulting solution with the electrode at 4 °C for 12 h, the thiol groups at the 5′-terminus of the hairpin DNA formed Au-S bonds with the gold electrode. Afterwards, the DNA/gold electrode was incubated in 100 μL solution of 1 mM MCH for 2 h to block the residual gold electrode sites. MCH served as a spacer to modulate the surface density of hairpin DNA and remove the nonspecifically adsorbed hairpin DNA.

After formation of the DNA/MCH modified monolayer, the electrode was incubated in 20 μL of reaction mixture containing 1 × DSN master buffer (50 mM Tris-HCl, 5 mM $MgCl_2$, 1 mM DTT, pH 8.0), 0.2 U DSN and a given concentration of target miRNA (miRNA-21) at 60 °C in an enclosed environment for 50 min. Subsequently, 20 μL of 10 mM EDTA were added to the above reaction mixture and incubated at 60 °C for 5 min to deactive DSN enzyme.

After rinsing with water to remove any non-specifically adsorbed substances, the electrode was immersed in 30 μL of signal DNA solution (2 μM) at room temperature for 1 h. Next, the electrode was rinsed three times with 10 mM Tris-HCl buffer (pH 7.4). SA-AuNPs solution (15 μL, $A_{520} = 1.0$) was dropped onto the electrode and incubated at room temperature for 30 min, followed by rinsing three times with 10 mM Tris–HCl (pH 7.4). Then, 15 μL of 0.5 μg/mL Biotin-HRP solution was added on the electrode surface and incubated at room temperature for 45 min. The electrode was rinsed three times with 10 mM Tris–HCl (pH 7.4) and subjected to electrochemical measurement.

2.4. Cell culture and miRNA analysis in cell lysates

The human lung cancer cell line (A549 cells) were obtained from the cell bank of the type culture collection of the Chinese Academy of Sciences (Shanghai, China) and cultured in Dulbecco's modified Eagle medium (DMEM) with 10% fetal bovine serum (FBS) and 1% penicillin-streptomycin at 37 °C, 5% CO_2 in an incubator (Thermo Scientific). The cells were harvested after incubation for two days, and the cells were then washed with PBS (10 mM, pH 7.4) two times. To extract the RNA, the harvested cells were first recycled at 37 °C and liquid nitrogen for 3 min three times. A volume of 40 μL of chloroform and 200 μL of PBS (10 mM, pH 7.4) were then added into the cells lysates solution under violent shaking for 15 s. Afterward, the mixture was kept at room temperature for 3 min, and then centrifuged at 12 000 rpm for 15 min to collect the supernatant.

Then, 100 μL of isopropanol was added into the supernatant, and the mixture was kept at room temperature for 10 min. The RNA was precipitated by centrifugation at 13 000 rpm for 10 min, and the resulting RNA was redispersed in 30 μL of DEPC-treated water and the miRNA was further analyzed by using our proposed strategy. For miRNA-21 detection by qRT-PCR, we first converted miRNA into cDNA at 37 °C for 120 min (including the label of the 3′ with poly (A) tail, and subsequent reverse transcription) using the reverse transcription kit (Tiangen Biotechnologies Co., Ltd.). The obtained cDNA was amplified using the SYBR Green real-time PCR detection kit (Tiangen Biotechnologies Co., Ltd.).

3. Results and discussion

3.1. Feasibility of the electrochemical biosensor

In this paper, CV was utilized to observe the catalytic effect of HRP and the feasibility of this protocol (Fig. 2). In the absence of target miRNA-21, two pairs of well-defined redox peaks which were characteristic of the two-electron oxidation and reduction reactions of TMB could be observed [43]. In the presence of 100 fM target miRNA-21, the height of the reduction peak located at about 210 mV increased, leading to a pair of asymmetric redox peaks that were assigned to the electrocatalysis reaction of HRP. When the concentration of the target miRNA-21 was increased to 100 pM, more HRP could be immobilized on the surface of the electrode, and the electrochemical signal was obviously amplified by the catalytic reaction of H_2O_2. Here, TMB served as an electron shuttle, and its redox peaks increased obviously with more HRP catalyze the reduction of H_2O_2 [45,46]. The catalysis mechanism is presented in the following equations: (1)–(3).

$$HRP_{Red} + H_2O_2 \rightarrow HRP_{ox} + H_2O \quad (1)$$

$$HRP_{ox} + TMB_{Red} \rightarrow TMB_{ox} + HRP_{Red} \quad (2)$$

$$TMB_{ox} + e^- \rightarrow TMB_{Red} \quad (3)$$

3.2. Characterization of the biosensor fabrication

EIS is an effective technique for monitoring the features of modified electrodes [47]. Fig. 3 shows the Nyquist plots of impedance spectra corresponding to the different modified gold electrodes, and the inset shows the applied equivalent circuit. The charge transfer resistance (R_{et}) value of $[Fe(CN)_6]^{4-}/[Fe(CN)_6]^{3-}$ at bare gold electrode was about 200 Ω (curve a), implying a very small electron transfer resistance, which meant that $[Fe(CN)_6]^{4-/3-}$ could reach the electrode surface and exchange charge readily. After the immobilization of thiol-modified hDNA and blocking with MCH (curve b and curve c), the R_{et} increased to 3.7 kΩ and 4.76 kΩ, respectively, indicating that the DNA/MCH modified monolayers had been formed on the electrode. However, the R_{et} decreased to 1.72 kΩ when the electrode was treated with the miRNAs and DSN solution (curve d). This decrease in resistance could be ascribed to the successful digestion of the RNA/DNA duplexes by DSN. Subsequently, by hybridizing with the corresponding biotin-labeled sDNA, the R_{et} increased again because of the increased steric hindrance effect (curve e). Finally, after the as-prepared biosensor was incubated with SA-AuNPs and the biotin-HRP, the R_{et} increased step by step (curve f and curve g), which implied that the nonconductive proteins obstructed electron transfer severely and prevented the $[Fe(CN)_6]^{4-/3-}$ redox probe from reaching the electrode surface.

3.3. Optimization of the experimental condition

Because the DSN amplification strategy is the key parameter for the sensitivity of the miRNA biosensor, the experimental variables in this strategy, including the amount of DSN enzyme, the incubation time and the working temperature were considered and optimized. As Fig. 4A shows, with increasing amounts of DSN, the current change (Δi) increased rapidly at low amounts, then increased slowly and reached a plateau at 0.2 U. Thus, the 0.2 U DSN was chosen as the optimal amount in subsequent measurements. The effect of incubation time on the current intensity was also investigated. As illustrated in Fig. 4B, Δi successively increased up to 50 min incubation time, and then there was no significant current variation with prolonged enzyme system reaction time, indicating that 50 min was the optimal incubation time. DSN is stable in a wide pH range from 4 to 12 and has a broad working temperature range below 65 °C [30–41]. Thus, the working temperature of the DSN was fixed at its optimal temperature of 60 °C in this work (Fig. 4C).

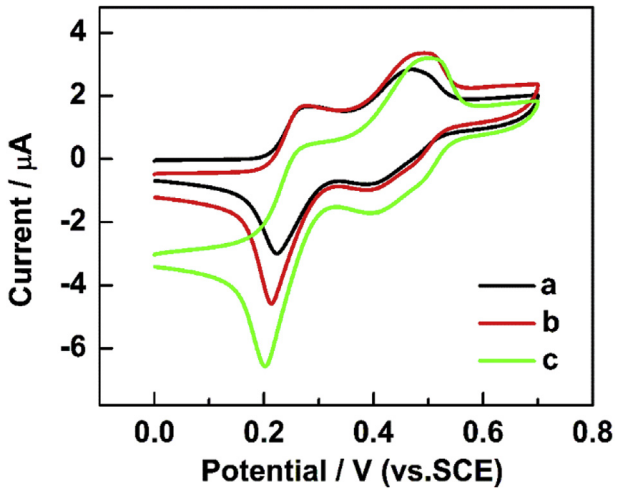

Fig. 2. Cyclic voltammograms of the electrochemical biosensor monitoring the TMB redox reaction in the presence of (a) 0 M, (b) 100 fM and (c) 100 pM miRNA-21.

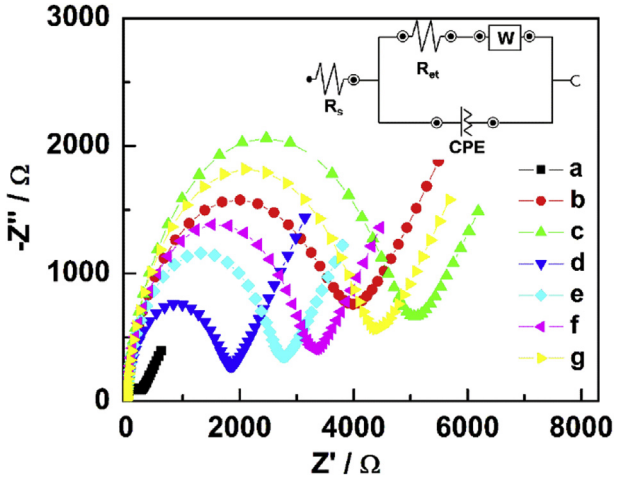

Fig. 3. Nyquist plot of different modified gold electrodes: (a) bare gold electrode; (b) hDNA modified gold electrode; (c) MCH blocked hDNA modified gold electrode; (d) treated in the miRNA-21 and DSN solution; (e) incubated with biotin-labeled sDNA; (f) incubated with SA-AuNPs and (g) biotin-HRP.

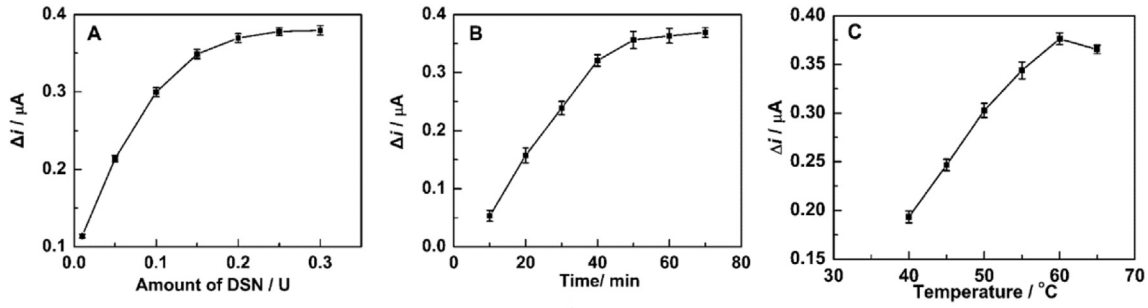

Fig. 4. Influence of (A) the concentration of DSN, (B) incubation time and (C) the working temperature on the current response of the electrochemical biosensor. The concentrations of miRNAs were all 100 fM.

3.4. Sensitivity of the electrochemical biosensor to miRNA-21

Amperometry provides a simple and direct way to characterize the enzyme-catalyzed electrochemical reaction. Under the optimal conditions, the sensitivity of this protocol to miRNA-21 detection was demonstrated. Upon the onset of the potential at 100 mV, the current–time (*i*-t) decay curves could be observed immediately, and they reached a plateau (steady-state current) within 100 s (Fig. 5). The background current of the biosensor was as low as 5 nA (in the absence of miRNA-21), suggesting that there was little non-specific binding of either sDNA strands or the enzyme. We also found that the amperometric current was related to the concentration of miRNA-21.

The current variation increased monotonically with the logarithm of the concentration of miRNA-21, resulting in a typical dose–response curve. The inset in Fig. 5 shows a broad linear relationship between the amperometric current change Δi and the logarithm of the concentration of miRNA-21 in the range of 0.1 fM~100 pM with a correlation coefficient (R) of 0.997, and the linear fitting equation is Δi (μA) = 0.1239 logc (fM)+0.1391, where Δi is the amperometric current change ($\Delta i = i\text{-}i_0$, where i and i_0 represent the amperometric currents in the presence and absence of miRNA-21, respectively), and c is the concentration of miRNA-21. This method belongs to the "signal-on" biosensor, which exhibits intrinsic merits such as over traditional "signal-off" mode. The detection limit of the method, estimated from the signal/noise of 3, was 43.3 aM, which is lower than that of many previously reported assays for miRNA determination [19,21–25,30,32,33,35,40,41,46,48], as shown in Table 1. The lower detection limit can be attributed to the DSN assisted recycling and the signal amplification of Au NPs and HRP.

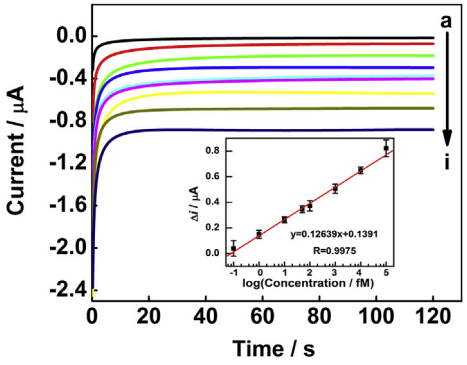

Fig. 5. Amperometric currents of the electrochemical biosensor in response to the concentration of miRNA-21, the concentration for the curves (a) to (i) is 0, 0.1 fM, 1 fM, 10 fM, 50 fM, 100 fM, 1 pM, 10 pM, 100 pM, respectively. The inset is the linear calibration curve of Δi value versus the logarithm of the concentration of miRNA-21.

3.5. Selectivity and reproducibility of the electrochemical biosensor

For a miRNA biosensor, the detection specificity is also an important parameter. The specificity of this method was evaluated by measuring the amperometric current response of the electrochemical biosensor to different types of miRNA sequences, including target miRNA-21 (S1), one-base mismatched strand (S2), three-base mismatched strand (S3) and random non-complementary strand (S4). As shown in Fig. 5, the current differences of the four types of miRNAs sequences were obvious. Although the amperometric current of the one-base mismatched microRNA-21 (S2) also could be observed ($\Delta i = 0.027$ μA), it was not comparable with that of the miRNA-21 (S1) ($\Delta i = 0.398$ μA). The results demonstrated that the proposed miRNA biosensor could offer high specificity in discriminating target and mismatched miRNA, as a result of the powerful discriminating ability of hDNA and DSN.

The repeatability of the biosensor was estimated by analyzing five independently fabricated biosensors toward 1 pM miRNA-21. The relative standard deviation (RSD) of the slope of the calibration plot was about 5.2%, revealing a desirable repeatability and precision of this method.

3.6. Detection of miRNA-21 in A549 cell lysates

To evaluate the feasibility of our proposed strategy for real sample detection, the expression of miRNA-21 in A549 tumor cells (a cell line with high expression of miRNA-21) were investigated by the electrochemical biosensor. The cell extractions were processed after cell counting and were measured by our method and a commercial qRT-PCR kit simultaneously. As shown in Fig. 6B, the copies of miRNA-21 increased obviously when the cells amount increased from 10^2 cells to 10^6 (gray bars, Fig. 6B). Compared with referenced qRT-PCR results (red bars, Fig. 6B), the concentration of endogenous miRNA-21 of A549 cells detected by the biosensor and qRT-PCR kit were in good agreement with each other (Fig. 6B). Therefore, the proposed biosensor allowed detection of miRNA in real samples and had promising potential in clinical diagnosis.

4. Conclusion

In summary, we developed a highly sensitive electrochemical biosensor for miRNA detection. The miRNA biosensor was based on a triple signal amplification strategy, which combined Au NPs improved enzyme loading and electrical communication between HRP and electrode, HRP enzymatic signal amplification and DSN

Table 1
Analytic performance of diverse methods for miRNA detection.

Detection Method	Signal Amplification Strategy	Linear Range (fM)	Detection Limit (fM)	Ref.
fluorescence	DSN-assisted target recycling	1×10^5–1×10^8	1×10^2	[32]
fluorescence	DSN-assisted target recycling	5×10^2–5×10^5	4×10^2	[35]
fluorescence	WS_2 Nanosheet and DSN-assisted target recycling	1×10^3–1×10^7	3×10^2	[40]
electrochemical	Au NPs and enzymes	1×10^1–7×10^5	6	[19]
electrochemical	Oligonucleotide encapsulated Ag nanoclusters	1×10^2–1×10^7	67	[21]
electrochemical	Au NPs, enzymes and redox-cycling reaction	10–5×10^3	3	[22]
electrochemical	DSN-assisted target recycling	2–2×10^3	1	[23]
electrochemical	programmable hairpin probe	10–5×10^3	2.56	[24]
electrochemical	rolling circle amplification and nanoelectrocatalysis	1–2×10^6	0.3	[25]
electrochemical	Au NPs/MoS_2 microcubes, enzymes and DSN-assisted target recycling	0.1–1×10^2	0.086	[30]
electrochemical	DSN-assisted target recycling	5–5×10^4	3.0	[33]
electrochemical	DNA tetrahedron structured probes and DSN-assisted target recycling	0.2–2×10^3	0.0178	[34]
electrochemical	MNPs-Au NPs-CdS NPs and DSN-assisted target recycling	1–1×10^5	0.48	[41]
electrochemical	DNA nanostructure and enzyme	1–1×10^6	0.1	[46]
electrochemical	Au NPs, iridium (III) complex and G-quadruplex	5–1×10^3	1.6	[48]
electrochemical	Au NPs, enzymes and DSN-assisted target recycling	0.1–1×10^5	0.043	current paper

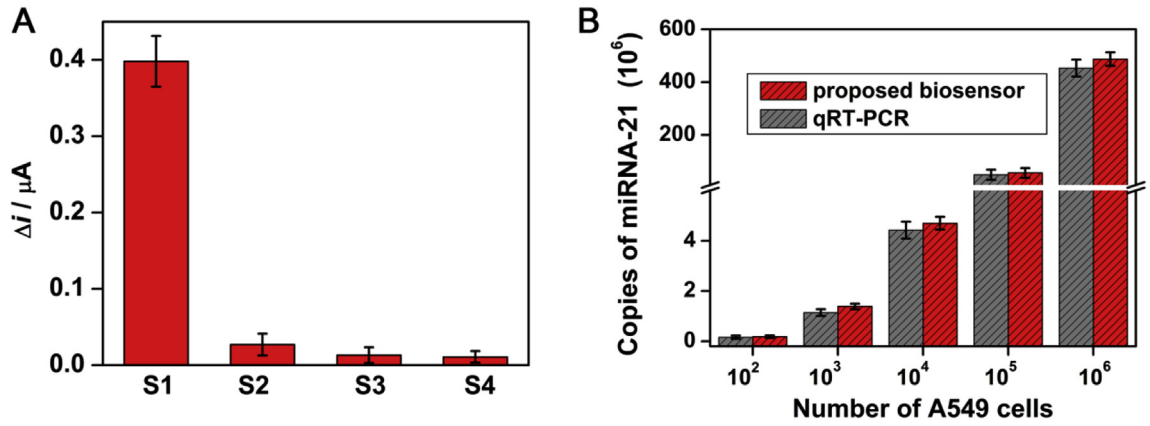

Fig. 6. (A) Selectivity of the biosensor toward miRNA-21 (S1) and base-mismatched miRNA (S2, S3, and S4). The concentrations of miRNAs were all 100 fM. (B) Measurement of the amount of miRNA-21 in A549 cells by our proposed biosensor and qRT-PCR.

assisted target recycling amplification. It was demonstrated that the value of the amperometric current change had a good linear relationship with the logarithm of the concentration of miRNA-21. More importantly, by taking advantage of the great discriminating ability of hDNA and DSN, the method could differentiate miRNAs sequences with one base difference. The proposed protocol exhibited great precision, high selectivity and good repeatability for miRNA detection, and the concentration of endogenous miRNA-21 of A549 cells can be detected with good result, thus providing a novel platform for miRNA analysis and clinical diagnosis. Furthermore, this method can be further applied for the detection of other miNRA by adapting their corresponding nucleotide probes and has great potential application in biomedical research.

Acknowledgements

We are grateful to the financial support of the National Natural Science Foundation of China (21375063 and 21575069), the Natural Science Foundation of Jiangsu Province (BK20181382) and the Jiangsu Collaborative Innovation Center of Biomedical Functional Materials.

References

[1] M.V. Iorio, C.M. Croce, MicroRNAs in cancer: small molecules with a huge impact, J. Clin. Oncol. 27 (2009) 5848–5856.
[2] J.C. Brase, D. Wuttig, R. Kuner, H. Sültmann, Serum microRNAs as non-invasive biomarkers for cancer, Mol. Canc. 9 (2010) 306–314.
[3] G.A. Calin, C.M. Croce, MicroRNA signatures in human cancers, Nat. Rev. Canc. 6 (2006) 857–866.
[4] A. Esquela-Kerscher, F.J. Slack, Oncomirs–microRNAs with a role in cancer, Nat. Rev. Canc. 6 (2006) 259–269.
[5] P.S. Mitchell, R.K. Parkin, E.M. Kroh, B.R. Fritz, S.K. Wyman, E.L. Pogosova-Agadjanyan, A. Peterson, J. Noteboom, K.C. O'Briant, A. Allen, D.W. Lin, N. Urban, C.W. Drescher, B.S. Knudsen, D.L. Stirewalt, R. Gentleman, R.L. Vessella, P.S. Nelson, D.B. Martin, M. Tewari, Circulating microRNAs as stable blood-based markers for cancer detection, Proc. Natl. Acad. Sci. U. S. A. 105 (2008) 10513–10518.
[6] L. Soleymani, Z. Fang, E.H. Sargent, S.O. Kelley, Programming the detection limits of biosensors through controlled nanostructuring, Nat. Nanotechnol. 4 (2009) 844–848.
[7] C. Arenz, MicroRNAs-future drug targets? Angew. Chem. Int. Ed. 45 (2006) 5048–5050.
[8] S.D. Fiedler, M.Z. Carletti, L.K. Christenson, Quantitative RT-PCR methods for mature microRNA expression analysis, Methods Mol. Biol. 630 (2010) 49–64.
[9] L.P. Lim, N.C. Lau, P. Garrett-Engele, A. Grimson, J.M. Schelter, J. Castle, D.P. Bartel, P.S. Linsley, J.M. Johnson, Microarray analysis shows that some microRNAs downregulate large numbers of target mRNAs, Nature 433 (2005) 769–773.
[10] A. Válóczi, C. Hornyik, N. Varga, J. Burgyán, S. Kauppinen, Z. Havelda, Sensitive and specific detection of microRNAs by northern blot analysis using LNA-modified oligonucleotide probes, Nucleic Acids Res. 32 (2004) 175–181.
[11] K.A. Cissell, S. Shrestha, S.K. Deo, MicroRNA detection: challenges for the analytical chemist, Anal. Chem. 79 (2007) 4754–4761.
[12] N. Hao, P.P. Dai, T. Yu, J.J. Xu, H.Y. Chen, A dual target-recycling amplification strategy for sensitive detection of microRNAs based on duplex-specific nuclease and catalytic hairpin assembly, Chem. Commun. 51 (2015) 13504–13507.
[13] H.V. Tran, B. Piro, S. Reisberg, L.D. Tran, H.T. Duc, M.C. Pham, Label-free and reagentless electrochemical detection of microRNAs using a conducting polymer nanostructured by carbon nanotubes: application to prostate cancer biomarker miR-141, Biosens. Bioelectron. 49 (2013) 164–169.

[14] W. Pan, T.T. Zhang, H.J. Yang, W. Diao, N. Li, B. Tang, Multiplexed detection and imaging of intracellular mRNAs using a four-color nanoprobe, Anal. Chem. 85 (2013) 10581–10588.
[15] E. Paleček, M. Bartošík, Electrochemistry of nucleic acids, Chem. Rev. 112 (2012) 3427–3481.
[16] H. Xie, C.Y. Zhang, Z.Q. Gao, Amperometric detection of nucleic acid at femtomolar levels with a nucleic acid/electrochemical activator bilayer on gold electrode, Anal. Chem. 76 (2004) 1611–1617.
[17] J.P. Tosar, G. Brañas, J. Laíz, Electrochemical DNA hybridization sensors applied to real and complex biological samples, Biosens. Bioelectron. 26 (2010) 1205–1217.
[18] Q.M. Shen, M.X. Fan, Y. Yang, H. Zhang, Electrochemical DNA sensor-based strategy for sensitive detection of DNA demethylation and DNA demethylase activity, Anal. Chim. Acta 934 (2016) 66–71.
[19] H.S. Yin, Y.L. Zhou, C.X. Chen, L.S. Zhu, S.Y. Ai, An electrochemical signal 'off-on' sensing platform for microRNA detection, Analyst 137 (2012) 1389–1395.
[20] H.S. Yin, Y.L. Zhou, H.X. Zhang, X.M. Meng, S.Y. Ai, Electrochemical determination of microRNA-21 based on graphene, LNA integrated molecular beacon, AuNPs and biotin multifunctional bio bar codes and enzymatic assay system, Biosens. Bioelectron. 33 (2012) 247–253.
[21] H.F. Dong, S. Jin, H.X. Ju, K.H. Hao, L.P. Xu, H.T. Lu, X.J. Zhang, Trace and label-free microRNA detection using oligonucleotide encapsulated silver nanoclusters as probes, Anal. Chem. 84 (2012) 8670–8674.
[22] L. Liu, N. Xia, H.P. Liu, X.J. Kang, X.S. Liu, C. Xue, X.L. He, Highly sensitive and label-free electrochemical detection of microRNAs based on triple signal amplification of multifunctional gold nanoparticles, enzymes and redox-cycling reaction, Biosens. Bioelectron. 53 (2014) 399–405.
[23] Y.Q. Ren, H.M. Deng, W. Shen, Z.Q. Gao, A highly sensitive and selective electrochemical biosensor for direct detection of microRNAs in serum, Anal. Chem. 85 (2013) 4784–4789.
[24] J.Y. Zhuang, D.P. Tang, W.Q. Lai, G.N. Chen, H.H. Yang, Immobilization-free programmable hairpin probe for ultrasensitive electronic monitoring of nucleic acid based on a biphasic reaction mode, Anal. Chem. 86 (2014) 8400–8407.
[25] N. Yu, Z. Wang, C.C. Wang, J. Han, H.Y. Bu, Combining padlock exponential rolling circle amplification with $CoFe_2O_4$ magnetic nanoparticles for microRNA detection by nanoelectrocatalysis without a substrate, Anal. Chim. Acta 962 (2017) 24–31.
[26] H.F. Dong, X.D. Meng, W.H. Dai, Y. Cao, H.T. Lu, S.F. Zhou, X.J. Zhang, Highly sensitive and selective microRNA detection based on DNA-bio-bar-code and enzyme-assisted strand cycle exponential signal amplification, Anal. Chem. 87 (2015) 4334–4340.
[27] M. Wang, Z.L. Fu, B.C. Li, Y.L. Zhou, H.S. Yin, S.Y. Ai, One-step, ultrasensitive, and electrochemical assay of microRNAs based on T7 exonuclease assisted cyclic enzymatic amplification, Anal. Chem. 86 (2014) 5606–5610.
[28] J.R. Yang, M. Tang, W. Diao, W.B. Cheng, Y. Zhang, Y.R. Yan, Electrochemical strategy for ultrasensitive detection of microRNA based on MNAzyme-mediated rolling circle amplification on a gold electrode, Microchimica. Acta. 183 (2016) 3061–3067.
[29] H.F. Dong, J.P. Lei, L. Ding, Y.Q. Wen, H.X. Ju, X.J. Zhang, MicroRNA: function, detection, and bioanalysis, Chem. Rev. 113 (2013) 6207–6233.
[30] H.L. Shuai, K.J. Huang, Y.X. Chen, L.X. Fang, M.P. Jia, Au nanoparticles/hollow molybdenum disulfide microcubes based biosensor for microRNA-21 detection coupled with duplex-specific nuclease and enzyme signal amplification, Biosens. Bioelectron. 89 (2017) 989–997.
[31] A.D. Castañeda, N.J. Brenes, A. Kondajji, R.M. Crooks, Detection of microRNA by electrocatalytic amplification: a general approach for single-particle, biosensing, J. Am. Chem. Soc. 139 (2017) 7657–7664.
[32] B.C. Yin, Y.Q. Liu, B.C. Ye, One-step, multiplexed fluorescence detection of microRNAs based on duplex-specific nuclease signal amplification, J. Am. Chem. Soc. 134 (2012) 5064–5067.
[33] C.Y. Yang, B.T. Dou, K. Shi, Y.Q. Chai, Y. Xiang, R. Yuan, Multiplexed and amplified electronic sensor for the detection of microRNAs from cancer cells, Anal. Chem. 86 (2014) 11913–11918.
[34] F. Xu, H.F. Dong, Y. Cao, H.T. Lu, X.D. Meng, W.H. Dai, X.J. Zhang, K.A. Al-Ghanim, S. Mahboob, Ultrasensitive and multiple disease-related microRNA detection based on tetrahedral DNA nanostructures and duplex-specific nuclease-assisted signal amplification, ACS Appl. Mat. Interfaces 8 (2016) 33499–33505.
[35] X.Y. Lin, C. Zhang, Y.S. Huang, Z. Zhu, X. Chen, C.J. Yang, Backbone-modified molecular beacons for highly sensitive and selective detection of microRNAs based on duplex specific nuclease signal amplification, Chem. Commun. 49 (2013) 7243–7245.
[36] S. Wang, B.S. Fu, Q. Wang, Y.L. Long, X.E. Zhang, S. Peng, P. Guo, T. Tian, X. Zhou, Novel amplex red oxidases based on noncanonical DNA structures: property studies and applications in MicroRNA detection, Anal. Chem. 86 (2014) 2925–2930.
[37] F. Degliangeli, P. Kshirsagar, V. Brunetti, P.P. Pompa, R. Fiammengo, Absolute and direct MicroRNA quantification using DNA–Gold nanoparticle probes, J. Am. Chem. Soc. 136 (2014) 2264–2267.
[38] J. Guo, C.J. Yuan, Q. Yan, Q.Y. Duan, X.L. Li, G. Yi, An electrochemical biosensor for microRNA-196a detection based on cyclic enzymatic signal amplification and template-free DNA extension reaction with the adsorption of methylene blue, Biosens. Bioelectron. 105 (2018) 103–108.
[39] S. Yu, Y.Y. Wang, L.P. Jiang, S. Bi, J.J. Zhu, Cascade amplification-mediated in situ hot-spot assembly for MicroRNA detection and molecular logic gate operations, Anal. Chem. 90 (2018) 4544–4551.
[40] Q. Xi, D.M. Zhou, Y.Y. Kan, J. Ge, Z.K. Wu, R.Q. Yu, J.H. Jiang, Highly sensitive and selective strategy for MicroRNA detection based on WS_2 nanosheet mediated fluorescence quenching and duplex-specific nuclease signal amplification, Anal. Chem. 86 (2014) 1361–1365.
[41] X.M. Li, L.L. Wang, J. Luo, Q.L. Wei, A dual-amplified electrochemical detection of mRNA based on duplex-specific nuclease and bio-bar-code conjugates, Biosens. Bioelectron. 65 (2015) 245–250.
[42] J. Jia, B. Wang, A. Wu, G. Cheng, L. Zhuang, S. Dong, A method to construct a third-generation horseradish peroxidase biosensor: self-assembling gold nanoparticles to three-dimensional sol-gel network, Anal. Chem. 74 (2002) 2217–2223.
[43] T.X. Hu, L. Zhang, W. Wen, X.H. Zhang, S.F. Wang, Enzyme catalytic amplification of miRNA-155 detection with graphene quantum dot-based electrochemical biosensor, Biosens. Bioelectron. 77 (2016) 451–456.
[44] J. Zhang, S.P. Song, L.H. Wang, D. Pan, C.H. Fan, A gold nanoparticle-based chronocoulometric DNA sensor for amplified detection of DNA, Nat. Protoc. 2 (2007) 2888–2895.
[45] E. Baldrich, F.J. del Campo, F.X. Munoz, Biosensing at disk microelectrode arrays. Inter-electrode functionalisation allows formatting into miniaturised sensing platforms of enhanced sensitivity, Biosens. Bioelectron. 25 (2009) 920–926.
[46] Y.L. Wen, H. Pei, Y. Shen, J.J. Xi, M.H. Li, N. Lu, X.Z. Shen, J.H. Li, C.H. Fan, DNA nanostructure-based interfacial engineering for PCR-free ultrasensitive electrochemical analysis of microRNA, Sci. Rep. 2 (2012) 867–872.
[47] K.J. Huang, D.J. Niu, Wa.Z. Xie, W. Wang, A disposable electrochemical immunosensor for carcinoembryonic antigen based on nano-Au/multi-walled carbon nanotubes–chitosans nanocomposite film modified glassy carbon electrode, Anal. Chim. Acta 659 (2010) 102–108.
[48] X.M. Miao, W.H. Wang, T.S. Kang, J.B. Liu, K.K. Shiu, C.H. Leung, D.L. Ma, Ultrasensitive electrochemical detection of miRNA-21 by using an iridium (III) complex as catalyst, Biosens. Bioelectron. 86 (2016) 454–458.